Published in final edited form as:
AJR Am J Roentgenol. 2009 January ; 192(1): 279–287. doi:10.2214/AJR.08.1205.

Quantitative Molecular Imaging of Viral Therapy for Pancreatic Cancer Using an Engineered Measles Virus Expressing the Sodium-Iodide Symporter Reporter Gene

Stephanie K. Carlson[1,2], **Kelly L. Classic**[3], **Elizabeth M. Hadac**[2], **David Dingli**[2,4], **Claire E. Bender**[1], **Bradley J. Kemp**[1], and **Stephen J. Russell**[2,4]

[1]Department of Radiology, Mayo Clinic, 200 First St. SW, Rochester, MN 55905.

[2]Division of Molecular Medicine, Mayo Clinic, Rochester, MN.

[3]Section of Safety and Security, Mayo Clinic, Rochester, MN.

[4]Division of Hematology, Mayo Clinic, Rochester, MN.

Abstract

OBJECTIVE—Our objectives were to, first, determine the oncolytic potential of an engineered measles virus expressing the sodium-iodide symporter gene (MV-NIS) for intratumoral (IT) therapy of pancreatic cancer and, second, evaluate NIS as a reporter gene for in vivo monitoring and quantitation of MV-NIS delivery, viral spread, and gene expression in this tumor model.

MATERIALS AND METHODS—Cultured human pancreatic cancer cells were infected with MV-NIS. Light microscopy, cell viability, and iodide uptake assays were used to confirm viral infection and *NIS* gene expression and function in vitro. Human pancreatic tumor xenografts were established in mice and infected via IT MV-NIS injections. NIS-mediated IT iodide uptake was quantitated by ^{123}I micro-SPECT/CT. IT MV-NIS infection was confrmed by immunohistochemistry of excised pancreatic xenografts. The oncolytic efficacy of MV-NIS was determined by measurement of tumor growth and mouse survival.

RESULTS—Infection of human pancreatic cancer cell lines with MV-NIS in vitro resulted in syncytia formation, marked iodide uptake, and ultimately cell death. Tumor xenografts infected with MV-NIS concentrated radioiodine, allowing serial quantitative imaging with ^{123}I micro-SPECT/CT. IT MV-NIS therapy of human pancreatic cancer xenografts resulted in a significant reduction in tumor volume and increased survival time of the treated mice compared with the control mice.

CONCLUSION—MV-NIS efficiently infects human pancreatic tumor cells and results in sufficient radioiodine uptake to enable noninvasive serial imaging and quantitation of the intensity, distribution, and time course of *NIS* gene expression. MV-NIS also shows oncolytic activity in human pancreatic cancer xenografts: Tumor growth is reduced and survival is increased in mice treated with the virus.

Keywords

gene therapy; measles virus; micro-SPECT/CT; molecular imaging; pancreatic cancer; sodium-iodide symporter; viral therapy

Address correspondence to S. K. Carlson (E-mail: scarlson@mayo.edu).

S. J. Russell is inventor of MV-NIS and Mayo Clinic holds patents on the use of the measles virus for cancer therapy.

Pancreatic cancer is the fourth most frequent cause of cancer-related deaths in the United States [1]. Currently, the only curative option is early surgical resection in patients with localized disease. Owing to the invasive nature of the disease and lack of early specific symptoms, approximately 40–50% of patients have locally advanced disease at diagnosis [2]. In addition, there is a high risk of locoregional recurrence after surgical resection [2]. Traditional treatment options for locally advanced or recurrent pancreatic cancer have had little impact on the disease course, with a median patient survival of 10 months [2]. Therefore, the development of alternative locoregional therapies is needed.

Pancreatic adenocarcinoma is a hypovascular fibrotic tumor that prevents adequate intratumoral (IT) concentrations of systemically delivered drugs because of high interstitial pressure gradients [3,4]. Previous molecular therapy studies have shown that IT administration achieves a higher IT concentration of the active agent than IV or intraperitoneal delivery [3, 5]. Because pancreatic cancer has the propensity for local invasion, a targeted IT approach to therapy may improve local tumor control.

Replicating viruses have considerable potential as oncolytic agents. In particular, attenuated measles virus of the Edmonston lineage (MV-Edm) has substantial antitumor activity in multiple tumor cell types but produces minimal damage in normal cells [6–11]. MV-Edm causes a potent cytopathic effect as a result of massive cell–cell fusion (syncytia formation) mediated by two measles virus proteins, hemagglutinin (H) and membrane fusion (F) proteins [6,7,10]. A property of MV-Edm that distinguishes it from the wild-type measles virus is its ability to enter cells efficiently through the CD46 receptor [6,7,12]. The oncolytic specificity of MV-Edm results from its ability to discriminate the differential expression of CD46 in tumor cells and normal cells [12]. The CD46 receptor is strongly expressed in human pancreatic cancer cells [12], which makes pancreatic cancer a potentially attractive target for MV-Edm virotherapy.

The ability to monitor viral delivery and antitumor efficacy noninvasively is made possible by genetically modifying the virus to express a reporter gene that can be detected by molecular imaging techniques. The sodium-iodide symporter (NIS) gene is expressed as a protein on the surface of thyroid follicular cells and mediates uptake and concentration of iodide [13]. NIS has been used routinely for more than 50 years for noninvasive imaging and therapy of thyroid cancer. The human *NIS* gene was cloned in 1996 [14] and can be transferred to nonthyroid cells. Transfer of NIS to nonthyroid cells induces iodide uptake similar to or greater than that seen in cultured thyroid cells [8,11,15–19]. Preclinical studies have shown that transient and stable *NIS* expression by multiple tumor cell types stimulates significant iodide uptake in vitro and in vivo, allowing ^{123}I imaging with planar and SPECT and ^{124}I imaging with PET techniques [8,11,15–17,20].

Given the strong oncolytic potential of MV-Edm and the ability of NIS to serve as a reporter gene for iodine-based imaging and therapy, an engineered attenuated measles virus expressing the *NIS* gene (MV-NIS) was developed at our institution [8]. Our study objectives were to determine the efficacy of IT MV-NIS therapy for the treatment of pancreatic cancer and to evaluate the use of NIS as a reporter gene for monitoring and quantitation of MV-NIS delivery, viral spread, and gene expression in this cancer model.

Materials and Methods

Cell Culture

The following experiments used the BxPC-3, MiaPaCa-2, and Panc-1 human pancreatic cancer cell lines, and African green monkey kidney (Vero) cells purchased from the American Type Culture Collection. BxPC-3 cells were maintained in RPMI 1640 medium supplemented with

10% fetal bovine serum (FBS) and penicillin and streptomycin. MiaPaCa-2 and Panc-1 cells were maintained in Dulbecco's modified Eagle's medium supplemented with 10% FBS and penicillin and streptomycin. Vero cells were maintained in Dulbecco's modified Eagle's medium supplemented with 5% FBS and penicillin and streptomycin.

MV-NIS

A recombinant measles virus expressing the *NIS* gene was produced in our laboratory [8]. Briefly, the human NIS complementary DNA was amplified by polymerase chain reaction and cloned at different positions into the full-length infectious clone of MV-Edm. The virus that had the *NIS* gene inserted downstream of the *H* gene grew as efficiently as the parental virus MV-Edm. This virus was rescued, was efficiently amplified, and is now referred to as "MV-NIS" (Fig. 1). Attenuated measles virus coding for green fluorescent protein (MV-eGFP) was also constructed and rescued to facilitate in vitro cell infection and cell viability studies.

MV-NIS Infection of Pancreatic Cancer Cells In Vitro

MV-eGFP and MV-NIS were used to infect cultured BxPC-3, MiaPaCa-2, and Panc-1 human pancreatic cancer cells and control Vero cells. The tumor cells were plated in a 12-well plate the day before infection at a density of 1.5×10^5 cells per well. When the cells were approximately 60% confluent, the appropriate medium and various multiplicities of infection (MOIs) of virus (0.001, 0.01, 0.1) were added to each well. Infected cells were followed for 4 days by light and fluorescence microscopy to evaluate for syncytia formation.

Cell viability assays (CellTiter-Blue Cell Viability Assay, Promega) were performed 6 days after infection. This assay provides a fluorometric method for estimating the number of viable cells present in multiwell plates. Reagent (CellTiter-Blue Reagent, Promega) was added to the infected cultured pancreatic cancer cells and incubated at 37°C for 4 hours to allow cells to convert resazurin (a redox dye) into resorufin (a fluorescent end product). The fluorescent signal was measured by a fluorometer. There is a linear relationship between cell number and fluorescence. Results were normalized to the uninfected control for each cell line. Viable cells retain the ability to reduce resazurin into resorufin. Nonviable cells rapidly lose metabolic capacity and therefore do not reduce the indicator dye or generate a fluorescent signal.

^{125}I Uptake Assay

To determine whether human pancreatic cancer cells infected with MV-NIS could concentrate radioiodine in vitro, an iodide uptake study was performed [8]. BxPC-3 cells were plated overnight on 12-well plates (1.5×10^5 cells per well), infected with MV-NIS (MOIs = 0.01, 0.1, 1.0), and followed as the infection spread through the culture. Infected cells were washed with Hanks balanced salt solution and incubated at 37°C in 1 mL of medium containing Hanks balanced salt solution with HEPES (4-(2-hydroxyethyl)-1-piperazine ethanesulfonic acid; pH = 7.3) and 2.9 kBq of ^{125}I-Na. Radionuclide uptake was determined after 45 minutes by washing the cells twice with 1 mL of cold Hanks balanced salt solution, lysing the cells by the addition of 1 mol/L of NaOH, and measuring retained iodide activity with a gamma counter. Iodide uptake was measured at 48, 72, and 96 hours. Experiments were performed in triplicate with or without 10 μmol/L potassium perchlorate ($KClO_4$), a competing substrate of NIS.

In Vivo Imaging and Quantitation of IT Radionuclide Uptake

Experiments were approved by and performed in accordance with the institutional animal care and use committee guidelines. We used 5- to 7-week-old female nude mice in all experiments. Mice were housed in a pathogen-free barrier facility with access to mouse chow and water ad libitum. To establish tumor models, 10^7 washed BxPC-3 tumor cells in 100 μL of phosphate-buffered saline (PBS) were implanted subcutaneously in the right flank of eight mice. Injections

were performed with a 25-gauge needle with the mice under general anesthesia with isoflurane inhalation. Tumor size was monitored daily with caliper measurements. Tumor volume was calculated with the following formula:

$$V(\mathrm{mm}^3)=L \times W^2 \times 0.52,$$

where L is the maximum length and W is the maximum width of the tumor [16]. When tumor diameters reached approximately 7 mm, MV-NIS (3.5×10^6 tissue culture infective dose [$TCID_{50}$]) in 100 μL of Opti-MEM (Invitrogen) was injected IT in six mice. Two mice (controls) were injected IT with Opti-MEM only. Mice were observed daily and sacrificed by the American Veterinary Medicine Association recommended procedure of CO_2 gas inhalation at the end of the experiments or immediately if they met sacrifice criteria (≥ 15% loss of body weight, inability to eat or drink, tumor ulceration, or tumor burden exceeding 10% of total body weight).

All mice were maintained on a low-iodine diet and received thyroxine supplementation (5 mg/L) in their drinking water. This regimen maximizes iodide uptake by NIS-positive tumors while reducing thyroid gland uptake [17]. On days 2, 3, 5, and 8 after virus injection, the mice underwent radionuclide planar and micro-SPECT/CT to evaluate IT *NIS* gene expression and radioiodine uptake. Animals were anesthetized with intramuscular injection of ketamine (100 mg/kg) and xylazine (10 mg/kg) for imaging purposes. An 18.5-MBq (0.5-mCi) dose of ^{123}I was administered by intraperitoneal injection to all mice 45 minutes before imaging.

A high-resolution micro-SPECT/CT system (X-SPECT, Gamma Medica Ideas) was used for planar and fusion micro-SPECT/CT [21]. This system offers functional and anatomic imaging of small animals with a micro-SPECT resolution of approximately 3–4 mm using a parallel-hole collimator and a micro-CT resolution of approximately 155 μm. The coregistered CT and SPECT images are acquired without needing to remove the animal from the imaging system. A low-energy, high-resolution, parallel-hole collimator with a 12.5-cm field of view was used in all cases. The image acquisition time was 5 minutes for planar and 13 minutes for micro-SPECT (64 projections at 10 seconds per projection). Micro-CT image acquisition (155-μm slice thickness, 256 images) was performed in 1 minute at 0.25 mA and 80 kVp.

Quantitative analysis of all radionuclide images was performed by the first author using standardized techniques [21]. Whole-body activity (injected dose) in each mouse was determined by measuring activity in the syringe in a National Institute of Standards and Technology–calibrated dose calibrator before and after injection. Flank tumor activity was determined by region-of-interest (ROI) image analysis using software (PMOD Biomedical Image Quantification and Kinetic Modeling Software, PMOD Technologies) and previously validated image analysis techniques [21]. Briefly, all fused micro-SPECT/CT images were adjusted for equal image intensity, and multiple ROIs were drawn around the tumor margin on every CT image in which it was visualized, resulting in a volume of interest. Pixel counts in tumor regions were measured from the coregistered micro-SPECT images. Corresponding total IT pixel counts were converted to activity using the equations derived from scanning an ^{123}I standard containing a known amount of radioactivity [21]. Counts were corrected for radionuclide decay (^{123}I half-life = 13.2 hours), differences in image acquisition time, and background activity. Background activity was measured by ROI image analysis of the opposite normal control flank and subtracted from the MV-NIS-positive tumor activity measurements.

Immunohistochemistry of Pancreatic Tumor Xenografts

To confirm IT MV-NIS infection, measles nucleoprotein was detected by immunohistochemistry of frozen tissue sections obtained from the BxPC-3 xenografts. Fresh

snap-frozen samples were cut into 4-μm sections with a cryostat (model 1850, Leica) placed on charged slides (Fisherbrand Superfrost, Fisher), air dried, and fixed in cold acetone (4°C) for 10 minutes. Sections were incubated with 3% H_2O_2 in ethanol for 5 minutes to inactivate the endogenous peroxides. The slides were then incubated in 1:1,000 biotinylated mouse anti-MV-nucleoprotein antibody (MAB8906B, Chemicon International) for 60 minutes and rinsed with Tris (tris(hydroxymethyl)aminomethane and tris(hydroxymethyl)methylamine)-buffered saline tween (TBST) wash buffer. The slides were visualized using streptavidin peroxidase (P0397, DAKO-Cytomation) at a 1/300 dilution for 20 minutes. Sections were rinsed again with TBST wash buffer, incubated with a substrate (NovaRED substrate kit, Vector Laboratories) for 10 minutes, counterstained with modified Schmidt's hematoxylin for 5 minutes, rinsed in tap water for 3 minutes, dehydrated through graded alcohols, cleared in three changes of xylene, and mounted with a permanent mounting medium. For comparison, negative control tumors also underwent the same immunostaining procedure.

In Vivo MV-NIS Efficacy

Subcutaneous human pancreatic tumor xenografts (10^7 BxPC-3 tumor cells in 100-μL solution of PBS) were established in the right flanks of four groups of female nude mice (10 mice per group) (Fig. 2). Tumor size was monitored daily with caliper measurements. When the tumor diameters reached 5 mm, IT injections of either Opti-MEM medium (control group) or MV-NIS (3.5×10^6 $TCID_{50}$)/100-μL Opti-MEM) were given in one, three, or six doses administered 2 days apart. Tumor response was determined by daily serial measurements of tumor growth. The mice were killed if they met the sacrifice criteria described previously.

Statistical Analysis

Survival time was estimated from establishment of the human pancreatic cancer xenografts until mouse sacrifice using the Kaplan-Meier method. Survival curves were compared by the log-rank test with statistics software (GraphPad Prism, version 4.03, GraphPad Software) for Microsoft Windows to determine whether the treatment groups were significantly different from the control group and whether there was a statistically significant difference between the single and multiple IT MV-NIS injections. Mean tumor volumes in the treated mice versus the control mice were compared by the Student's *t* test until day 14 when the first of the 10 control mice was sacrificed because of tumor burden. Differences are considered statistically significant if $p < 0.05$.

Results

In Vitro MV-NIS Infection

Recombinant MV-NIS and MV-eGFP successfully infected all human pancreatic cancer cell lines tested. After infection, numerous giant multinucleated syncytia formed in the pancreatic cell cultures, eventually leading to cell death. Syncytia formation was detected as early as 24 hours after infection. Figure 3A shows massive syncytia formation in the BxPC-3 cell line 72 hours after infection with MV-eGFP. MTS (3-[4, 5-dimethylthiazol-2-yl]-5-[3-carboxymethoxyphenyl]-2[4-sulfophenyl]-2H-tetrazolium, inner salt) cell viability assays performed 6 days after infection revealed that the viability of the infected cells was greatly reduced in a dose-dependent manner (Fig. 3B).

In Vitro Iodide Uptake by MV-NIS–Infected Cells

Radionuclide uptake assays were performed 48, 72, and 96 hours after infection with MV-NIS to determine *NIS* expression and function. The peak iodide uptake in BxPC-3 human pancreatic cancer cells was 72 hours after MV-NIS infection (Fig. 4). This activity was nearly eliminated in the presence of $KClO_4$.

In Vivo Imaging and Quantitation of *NIS*-Expressing Pancreatic Cancer Xenografts

Planar and micro-SPECT/CT images showed the ability of *NIS*-expressing BxPC-3 pancreatic cancer xenografts to efficiently concentrate radioiodine in vivo, allowing noninvasive radionuclide imaging and quantitation of radionuclide uptake on days 2, 3, 5, and 8 after MV-NIS injection (Fig. 5). Serial images showed increasing or decreasing amounts of IT radionuclide uptake over time, reflecting increased or decreased MV-NIS replication and *NIS* gene expression [8]. ROI image analysis showed a wide variation of tumor activity in the virus-treated mice with an average injection dose per gram of tissue (% ID/g) of 11.4% ID/g (range, 4.3–22.1% ID/g) on day 2, 8.4% ID/g (range, 3–15.1% ID/g) on day 3, and 6.4% ID/g (range, 3.4–9.1% ID/g) on day 5. IT activity continued to decrease after day 5 (data not shown). Control tumor xenografts showed an average injection dose per gram of tissue of 2.8% ID/g (range, 2–3.4% ID/g).

NIS Gene Immunohistochemistry

Immunohistochemical staining of sections of the BxPC-3 human pancreatic tumor xenografts for measles virus nucleoprotein confirmed IT MV-NIS infection in all tumors injected with MV-NIS (Fig. 6). Control (MV-NIS-negative) tumors were negative for MV nucleoprotein immunoreactivity.

Efficacy of IT MV-NIS Therapy

IT therapy with MV-NIS significantly increased the survival time of the treated mice compared with control mice ($p = 0.005$ for all treated mice vs control mice, $p = 0.0003$ for the six-dose group vs the control group, and $p = 0.008$ for the three-dose and one-dose groups vs the control group) (Fig. 7). The median mouse survival time for the control group was 18 days (mean, 19 days; range, 14–29 days). The median mouse survival time for the treated mice was 33.5 days (mean, 34 days; range, 18–50 days) in dose group 1, 28.5 days (mean, 30 days; range, 15–90 days) in dose group 3, and 34 days (mean, 34 days; range, 18–50 days) in dose group 6.

There was a significant difference in tumor growth among the treatment groups with regard to the number of MV-NIS injections until day 14 after IT MV-NIS injection; however, there was no significant difference in survival among the treatment groups. IT MV-NIS therapy resulted in significant reduction in tumor growth in the treated mice compared with the control mice beginning on day 8 after tumor cell injection (5 days after IT MV-NIS injection) and persisting until approximately day 14. Although therapy with MV-NIS slowed the progression of pancreatic cancer xenografts, it did not lead to complete ablation of the tumors except in one mouse in dose group 3 that had complete tumor regression at sacrifice on day 90.

Discussion

MV-NIS has shown antitumor activity in several different preclinical tumor models [8,9,15]. There is also an ongoing phase I clinical trial using MV-NIS in patients with recurrent or refractory multiple myeloma at our institution; therefore, this agent is already available for clinical testing. In this study, we expanded the application of MV-NIS to determine its potential therapeutic efficacy against pancreatic adenocarcinoma.

Gene and viral therapy studies for pancreatic cancer have been promising in animals but ineffective in humans [3,22]. The reasons for human trial treatment failures are unknown but potentially are related to poor vector delivery to the target site or tumor resistance to therapy. Most previous human trials have not used molecular imaging techniques to monitor vector delivery and gene expression. A phase I clinical trial [3] tested the IT injection of an oncolytic adenovirus (ONYX-015) into primary pancreatic tumors and showed the safety and feasibility

of the technique; however, IT viral replication could not be detected and no objective tumor responses were observed [3]. The reasons for this were not clarified.

In most gene therapy trials to date, IT gene expression has been monitored by percutaneous needle aspiration or biopsy [3,23]. This can provide partial information, but it is invasive and subject to sampling error and serial biopsies in humans are generally not feasible. Noninvasive monitoring of gene expression and therapeutic response is critical to advance gene therapies in human subjects. For future translation to human trials, it would be desirable to monitor MV-NIS therapy with the most available and least costly radionuclide imaging technique. Currently, gamma planar imaging is more widely available clinically and is less expensive than cross-sectional imaging with SPECT or PET. However, pancreatic cancer poses a potential challenge for in vivo imaging with radioiodine-based techniques because of increased uptake of radioiodine in the stomach that may result in a strong signal on the radionuclide images. Because the pancreas lies in close proximity to the stomach, there is the potential for decreased spatial resolution and inaccurate monitoring of IT *NIS* expression. Cross-sectional fusion imaging techniques such as SPECT/CT and PET/CT are needed to improve 3D spatial resolution and separate the overlapping regions of radioiodine uptake in vivo.

The sensitivity of micro-SPECT/CT for imaging and quantitation of *NIS*-mediated radionuclide uptake has been established [19,21]. Marsee et al. [19] detected *NIS*-expressing orthotopic lung tumors as small (i.e., 3 mm) with micro-SPECT using pinhole collimation. Carlson et al. [21] showed that micro-SPECT/CT can be used to accurately quantify IT radionuclide uptake in vivo and is more reliable than planar or micro-SPECT alone. Quantitative indexes are necessary to more rapidly determine and monitor therapeutic efficacy in terms of response rates. SPECT/CT is already a widely used technique in humans; therefore, this method of in vivo gene monitoring is readily translatable to the clinic setting.

Radiology can advance cancer gene therapy by improving the delivery of therapeutic agents to target tissues. Imaging-guided, minimally invasive approaches are well suited for the IT delivery of gene therapy agents. Interventional radiologists can choose the site for targeted therapy and determine the best route of access allowing precise placement of the vectors in the target tissue, while minimizing the systemic toxic effects. Percutaneous IT injections can be performed safely using imaging guidance with CT, transcutaneous or endoscopic sonography, or MRI. The safety of direct IT and intraperitoneal injection of therapeutic agents has been proven in several clinical trials, including pancreatic cancer trials [3,23].

Circulating antimeasles-neutralizing antibodies can significantly accelerate the destruction of IV delivered MV-NIS in human subjects [8,9]. Therefore, IT injection techniques are essential for the delivery of MV-NIS to pancreatic tumors. Studies are under way in our laboratory to develop methods that will allow targeted systemic delivery of attenuated measles virus to immunocompetent patients and avoid destruction by the patient's immune system before reaching the target site [24]. These methods will be particularly useful in the treatment of metastatic disease.

In our study, there was no significant difference in survival among the treatment groups with regard to the number of MV-NIS injections. One would expect that as the dose of the virus in the tumor increased, cell death and mouse survival would also increase. There did appear to be a correlation between injection number and a reduction in tumor growth early in the study. However, we hypothesize that the first IT injection is critical for establishing homogeneous distribution of the therapeutic agent throughout the tumor and that additional injections may be able to slow growth of segments of the tumor, but that eventually the uninfected, rapidly growing portions of the tumor will overcome the areas of cell infection and death. As the uninfected portions of the tumor increase in size, the MOI in subsequent doses of virus is

smaller with regard to the remaining viable tumor volume. This finding emphasizes the importance of homogeneous IT distribution of the therapeutic agent to ensure eradication of the entire tumor volume. Alternately, as with any replication-competent virus, it is conceivable that the initial infection of the most susceptible cells in the tumor resulted in a large viral amplification such that subsequent injections represented only a small fraction of the total viral load.

The attenuated strain of measles virus (i.e., MV-Edm) has been used safely for human vaccination since 1963 and has shown considerable oncolytic activity against multiple human tumor cell lines in vitro and in vivo [4,6–8,10,24]. Virus-infected tumor cells fuse readily with their uninfected neighboring cells to form multinucleated syncytia that eventually die. The oncolytic potency of MV-Edm in different tumor cell lines is highly variable. Previous studies at our institution [6,8] have shown that the natural oncolytic activity of MV-Edm in certain human myeloma tumor xenografts was not always sufficient because some tumors persisted despite repeated high doses of virus. Some investigators hypothesize that the virus and the tumor reach a dynamic equilibrium in which cell replication is enough to compensate for the rate of new infection by the virus and natural cell death and thus both can coexist [25,26]. Our results indicate that although MV-NIS has the ability to slow tumor progression and increase the survival of mice with BxPC-3 pancreatic cancer xenografts, the tumors were not completely eradicated by the virus alone (except in one mouse whose tumor had completely regressed by the end of the study). This finding emphasizes the need for other strategies to further increase tumor cell killing and enhance the therapeutic efficacy of MV-NIS.

Transfer of the *NIS* gene to human tumor cells not only allows the ability to monitor noninvasively the distribution and expression of viral infection in vivo using radioiodine imaging techniques but also offers the potential for radiation therapy [8,15–17,27]. Studies have shown tumor regression in multiple *NIS*-expressing tumor models after the administration of a therapeutic dose of ^{131}I [8,9,15–17,28–32]. We plan to explore the utility of using ^{131}I radiovirotherapy with IT MV-NIS therapy to enhance the oncolytic potency of this therapy in human pancreatic cancer.

A limitation of our study was that it would have been helpful to have a control (uninfected) BxPC-3 tumor in the flank opposite the MV-NIS-infected tumor in the same mouse in our serial imaging experiment. Although the amount of IT activity in the uninfected tumors in the control mice was significantly less than most of the MV-NIS-treated tumors, there is inherent radioiodine localization in any tumor secondary to the vascular supply and areas of blood pooling owing to necrosis. A more accurate calculation of *NIS*-specific IT activity in the infected tumors would have been obtained by subtracting the IT activity from an internal noninfected control tumor.

In conclusion, MV-NIS effectively infects human pancreatic cancer cells in vitro and in vivo and efficiently expresses the *NIS* gene, thereby allowing noninvasive and quantitative imaging of the distribution and time course of MV-NIS infection and *NIS* reporter gene expression. MV-NIS therapy is a promising alternative for patients with pancreatic cancer and warrants further investigation.

Acknowledgments

We thank our nuclear medicine technologist, Tracy Decklever, for technical expertise and imaging assistance. We also thank Alan Penheiter for assistance in preparation and critical review of this manuscript.

This work was supported by the National Cancer Institute (grants K08 CA103859-03A1 and R01 CA 100634-01), the Mayo Clinic SPORE in Pancreatic Cancer (grant P20 CA 102701), the Society of Gastrointestinal Radiology Research Grant Program, and the GE-AUR Radiology Research Academic Fellowship (GERRAF) Program.

References

1. American Cancer Society Website. www.cancer.org/docroot/STT/stt_0_2007.asp?sitearea=STT+level=1.. [Accessed October 28, 2008]. Cancer statistics for 2007.
2. Alberts S, Gores G, Kim G, et al. Treatment options for hepatobiliary and pancreatic cancer. Mayo Clin Proc 2007;82:628–637. [PubMed: 17493429]
3. Mulvihill S, Warren R, Venook A, et al. Safety and feasibility of injection with an E1B-55 kDa gene-deleted, replication-selective adenovirus (ONYX-015) into primary carcinomas of the pancreas: a phase I trial. Gene Ther 2001;8:308–315. [PubMed: 11313805]
4. Kuszyk BS, Corl FM, Franano FN, et al. Tumor transport physiology: implications for imaging and imaging-guided therapy. AJR 2001;177:747–753. [PubMed: 11566666]
5. Kondo Y, Chung YS, Sawada T, et al. Intratumoral injection of an Adriamycin immunoconjugate against human pancreatic cancer xenografts. Jpn J Cancer Res 1995;86:1072–1079. [PubMed: 8567399]
6. Peng KW, Ahmann GJ, Pham L, Greipp PR, Cattaneo R, Russell SJ. Systemic therapy of myeloma xenografts by an attenuated measles virus. Blood 2001;98:2002–2007. [PubMed: 11567982]
7. Peng K-W, TenEyck CJ, Galanis E, Kalli KR, Hartmann LC, Russell SJ. Intraperitoneal therapy of ovarian cancer using an engineered measles virus. Cancer Res 2002;62:4656–4662. [PubMed: 12183422]
8. Dingli D, Peng K, Harvey M, et al. Image-guided radiovirotherapy for multiple myeloma using a recombinant measles virus expressing the thyroidal sodium iodide symporter. Blood 2004;103:1641–1646. [PubMed: 14604966]
9. Blechacz B, Splinter P, Greiner S, et al. Engineered measles virus as a novel oncolytic viral therapy system for hepatocellular carcinoma. Hepatology 2006;44:1465–1477. [PubMed: 17133484]
10. Grote D, Russell S, Cornu T, et al. Live attenuated measles virus induces regression of human lymphoma xenografts in immunodeficient mice. Blood 2001;97:3746–3754. [PubMed: 11389012]
11. Hasegawa K, O'Connor M, Federspiel M, Russell S, Peng K. Dual therapy of ovarian cancer using measles viruses expressing carcinoembryonic antigen and sodium iodide symporter. Clin Cancer Res 2006;12:1868–1875. [PubMed: 16551872]
12. Anderson BD, Nakamura T, Russell SJ, Peng K-W. High CD46 receptor density determines preferential killing of tumor cells by oncolytic measles virus. Cancer Res 2004;64:4919–4926. [PubMed: 15256464]
13. Spitzweg C, Harrington KJ, Pinke LA, Vile RG, Morris JC. Clinical review 132: the sodium iodide symporter and its potential role in cancer therapy. J Clin Endocrinol Metab 2001;86:3327–3335. [PubMed: 11443208]
14. Dai G, Levy O, Carrasco N. Cloning and characterization of the thyroid iodide transporter. Nature 1996;379:458–460. [PubMed: 8559252]
15. Dingli D, Diaz R, Bergert E, O'Connor MK, Morris JC, Russell S. Genetically targeted radiotherapy for multiple myeloma. Blood 2003;102:489–496. [PubMed: 12649158]
16. Spitzweg C, Dietz AB, O'Connor MK, et al. In vivo sodium iodide symporter gene therapy of prostate cancer. Gene Ther 2001;8:1524–1531. [PubMed: 11704812]
17. Spitzweg C, O'Connor MK, Bergert ER, Tindall DJ, Young CYF, Morris JC. Treatment of prostate cancer by radioiodine therapy after tissue-specific expression of the sodium iodide symporter. Cancer Res 2000;60:6526–6530. [PubMed: 11103823]
18. Groot-Wassink T, Aboagye EO, Glaser M, Lemoine NR, Vassaux G. Adenovirus biodistribution and noninvasive imaging of gene expression in vivo by positron emission tomography using human sodium/iodide symporter as reporter gene. Hum Gene Ther 2002;13:1723–1735. [PubMed: 12396625]
19. Marsee DK, Shen DH, MacDonald LR, et al. Imaging of metastatic pulmonary tumors following *NIS* gene transfer using single photon emission computed tomography. Cancer Gene Ther 2004;11:121–127. [PubMed: 14730332]
20. Dingli D, Kemp BJ, O'Connor MK, Morris JC, Russell SJ, Lowe VJ. Combined I-124 positron emission tomography/computed tomography imaging of *NIS* gene expression in animal models of

stably transfected and intravenously transfected tumor. Mol Imaging Biol 2006;8:16–23. [PubMed: 16328647]

21. Carlson S, Classic K, Hadac E, et al. In vivo quantitation of intratumoral radioisotope uptake using micro-single photon emission computed tomography/computed tomography. Mol Imaging Biol 2006;8:324–332. [PubMed: 17053863]
22. Nemunaitis J, Ganly I, Khuri F, et al. Selective replication and oncolysis in *p53* mutant tumors with ONYX-015, an E1B-55kD gene-deleted adenovirus, in patients with advanced head and neck cancer: a phase II trial. Cancer Res 2000;60:6359–6366. [PubMed: 11103798]
23. Swisher SG, Roth JA, Nemunaitis J, et al. Adenovirus-mediated *p53* gene transfer in advanced non-small-cell lung cancer. J Natl Cancer Inst 1999;91:763–771. [PubMed: 10328106]
24. Hadac EM, Peng K-W, Nakamura T, Russell SJ. Reengineering paramyxovirus tropism. Virology 2004;329:217–225. [PubMed: 15518802]
25. Peng KW, Hadac EM, Anderson BD, et al. Pharmacokinetics of oncolytic measles virotherapy: eventual equilibrium between virus and tumor in an ovarian cancer xenograft model. Cancer Gene Ther 2006;13:732–738. [PubMed: 16543921]
26. Dingli D, Cascino MD, Josić K, Russell SJ, Bajzer Z. Mathematical modeling of cancer radiovirotherapy. Math Biosci 2006;199:55–78. [PubMed: 16376950]
27. Dingli D, Russell SJ, Morris JC 3rd. In vivo imaging and tumor therapy with the sodium iodide symporter. J Cell Biochem 2003;90:1079–1086. [PubMed: 14635183]
28. Chen L, Altmann A, Mier W, et al. Radioiodine therapy of hepatoma using targeted transfer of the human sodium/iodide symporter gene. J Nucl Med 2006;47:854–862. [PubMed: 16644756]
29. Dwyer RM, Bergert ER, O'Connor MK, Gendler SJ, Morris JC. In vivo radioiodide imaging and treatment of breast cancer xenografts after *MUC1*-driven expression of the sodium iodide symporter. Clin Cancer Res 2005;11:1483–1489. [PubMed: 15746050]
30. Dwyer RM, Bergert ER, O'Connor MK, Gendler SJ, Morris JC. Sodium iodide symporter-mediated radioiodide imaging and therapy of ovarian tumor xenografts in mice. Gene Ther 2006;13:60–66. [PubMed: 16121204]
31. Dwyer RM, Bergert ER, O'Connor MK, Gendler SJ, Morris JC. Adenovirus-mediated and targeted expression of the sodium-iodide symporter permits in vivo radioiodide imaging and therapy of pancreatic tumors. Hum Gene Ther 2006;17:661–668. [PubMed: 16776574]
32. Shimura H, Haraguchi K, Miyazaki A, Endo T, Onaya T. Iodide uptake and experimental I-131 therapy in transplanted undifferentiated thyroid cancer cells expressing the Na^{-}/I^{-}symporter gene. Endocrinology 1997;138:4493–4496. [PubMed: 9322970]

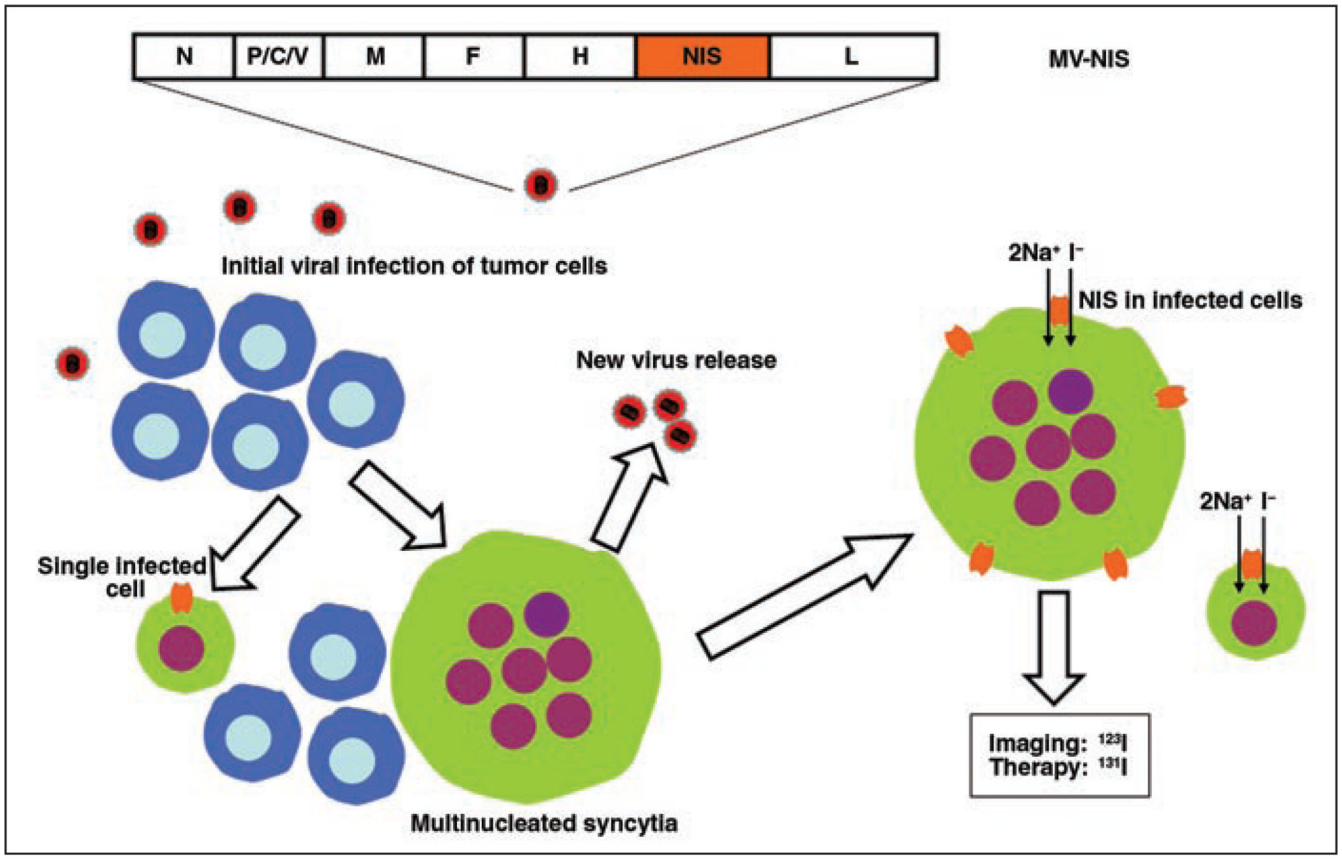

Fig. 1.

Schematic representation shows measles virus–sodium-iodide symporter (MV-NIS) genome and its function. Virus-infected tumor cells release new viral progeny and are able to fuse readily with their uninfected neighboring cells to form multinucleated syncytia that eventually die. Infection with MV-NIS also leads to membrane expression of NIS, which is intrinsic transmembrane protein normally expressed on basolateral surface of thyroid follicular cell that allows transport of one iodide ion and two sodium ions into cell. Significant intracellular iodide accumulation allows noninvasive imaging with radionuclide techniques and potential for targeted radiation therapy. N = nucleoprotein gene; P/C/V = phosphoprotein, C, and V genes; M = matrix protein gene; F = fusion protein gene; H = hemagglutinin gene; L = polymerase gene; Na^+ = sodium ion; I^- = iodide ion.

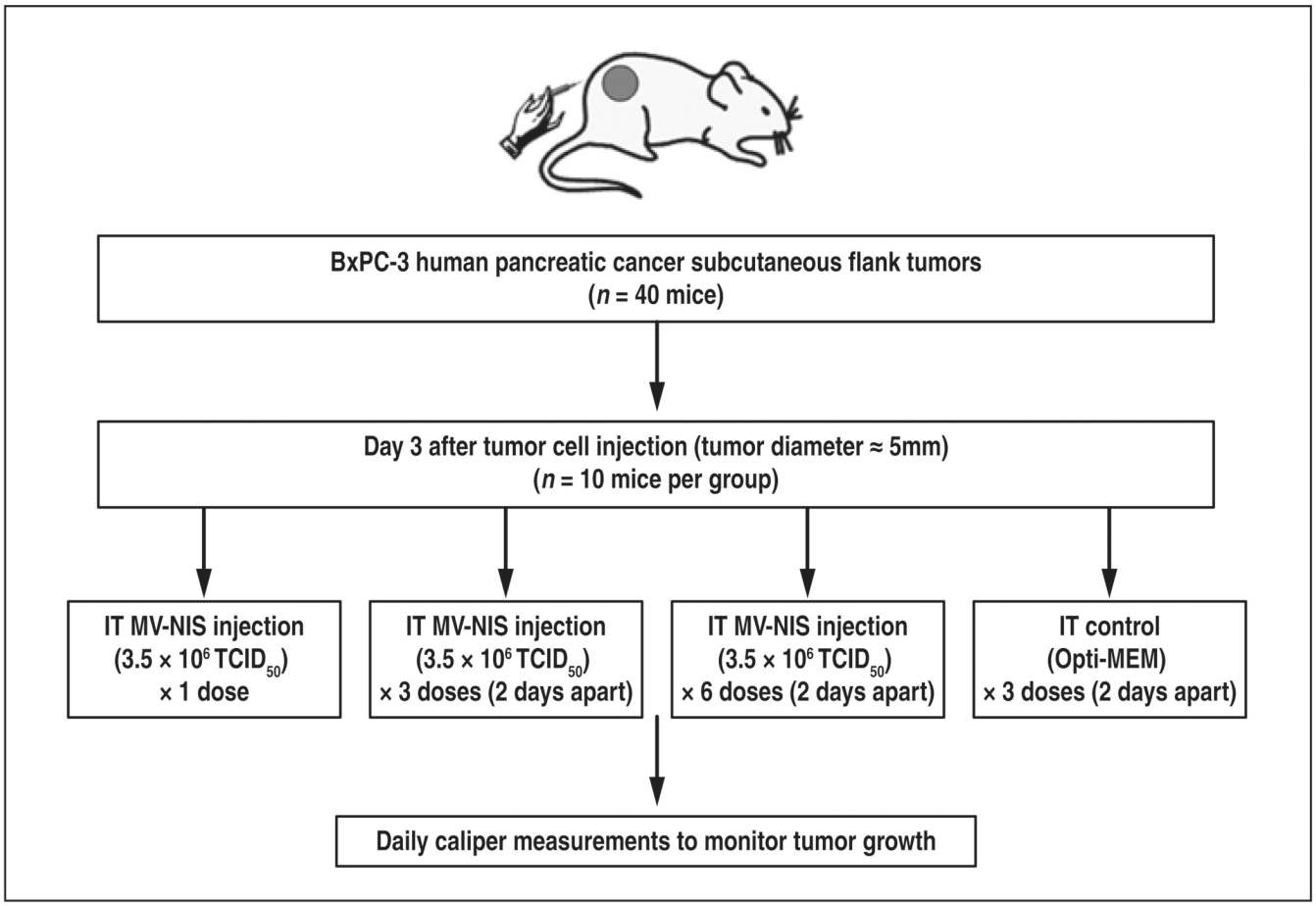

Fig. 2.

Diagram shows experimental design to study efficacy of engineered measles virus expressing sodium-iodide symporter gene (MV-NIS). IT = intratumoral, tissue culture infective dose ($TCID_{50}$). Opti-MEM manufactured by Invitrogen.

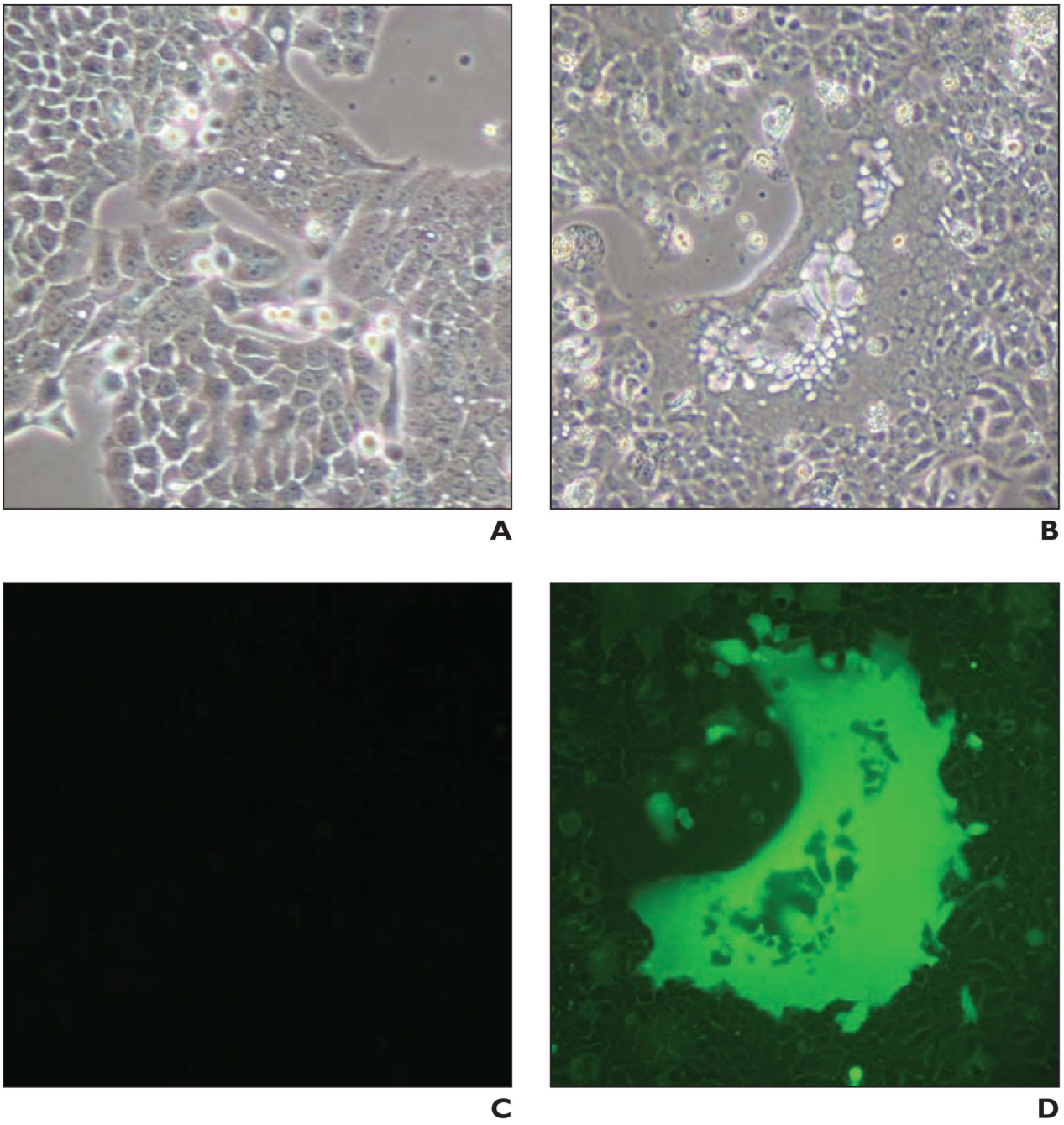

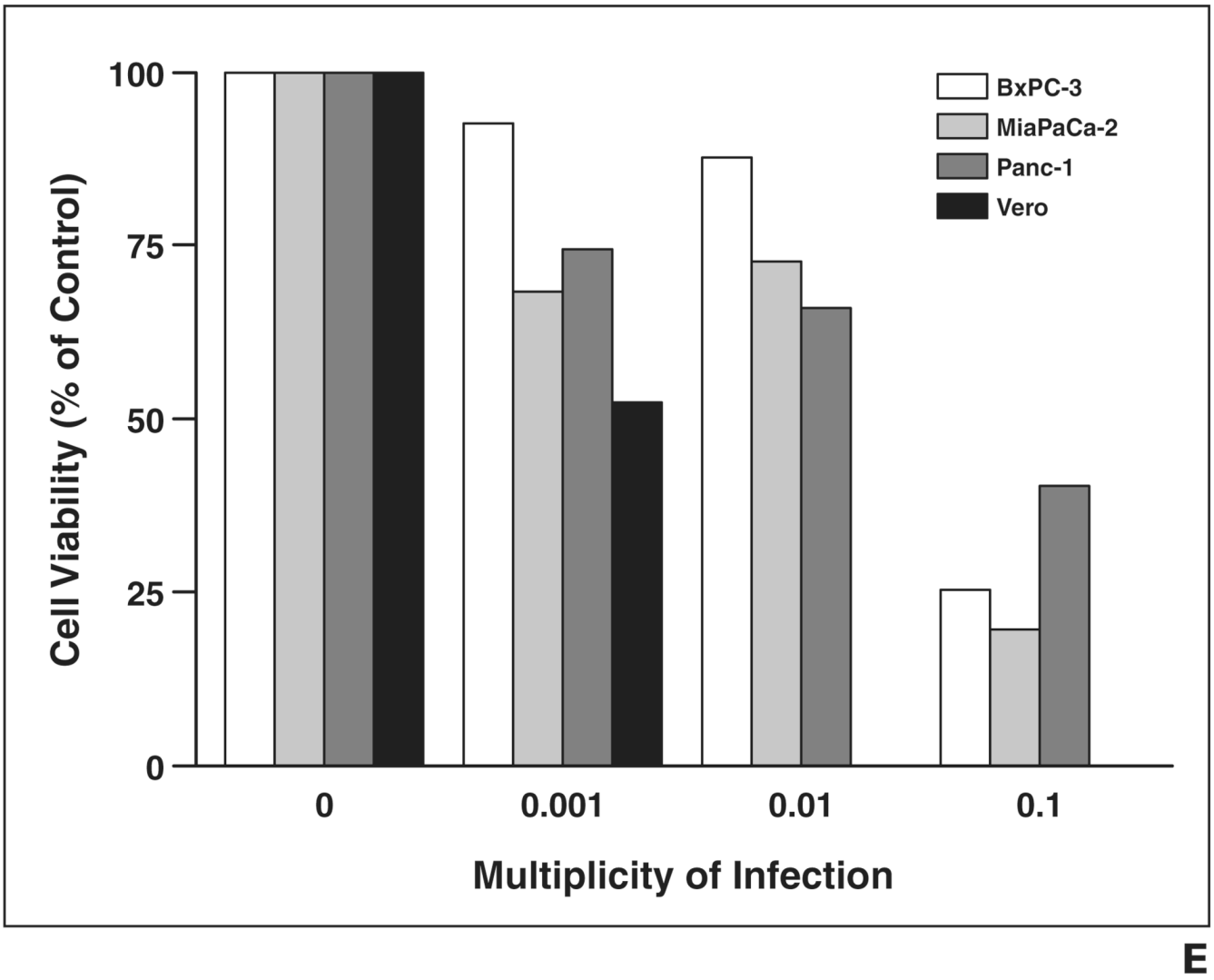

Fig. 3.

In vitro tumor cell infection studies.

A–D, Light (**A** and **B**) and fluorescence (**C** and **D**) micrograph images show uninfected (**A** and **C**) and infected (**B** and **D**) BxPC-3 cells. Infected BxPC-3 cells shown were infected with measles virus–enhanced green fluorescent protein (MV-eGFP; multiplicity of infection [MOI] = 0.1) and images were obtained 72 hours after infection. MV-eGFP and engineered measles virus expressing sodium-iodide symporter gene (MV-NIS) (images not shown) efficiently infect human pancreatic cancer cells, leading to syncytia and eventual cell death. **E,** MTS (3-[4, 5-dimethylthiazol-2-yl]-5-[3-carboxymethoxyphenyl]-2[4-sulfophenyl]-2H-tetrazolium, inner salt) cell viability assay 6 days after infection at various MOIs shows dose-dependent reduction in cell viability for all cell lines.

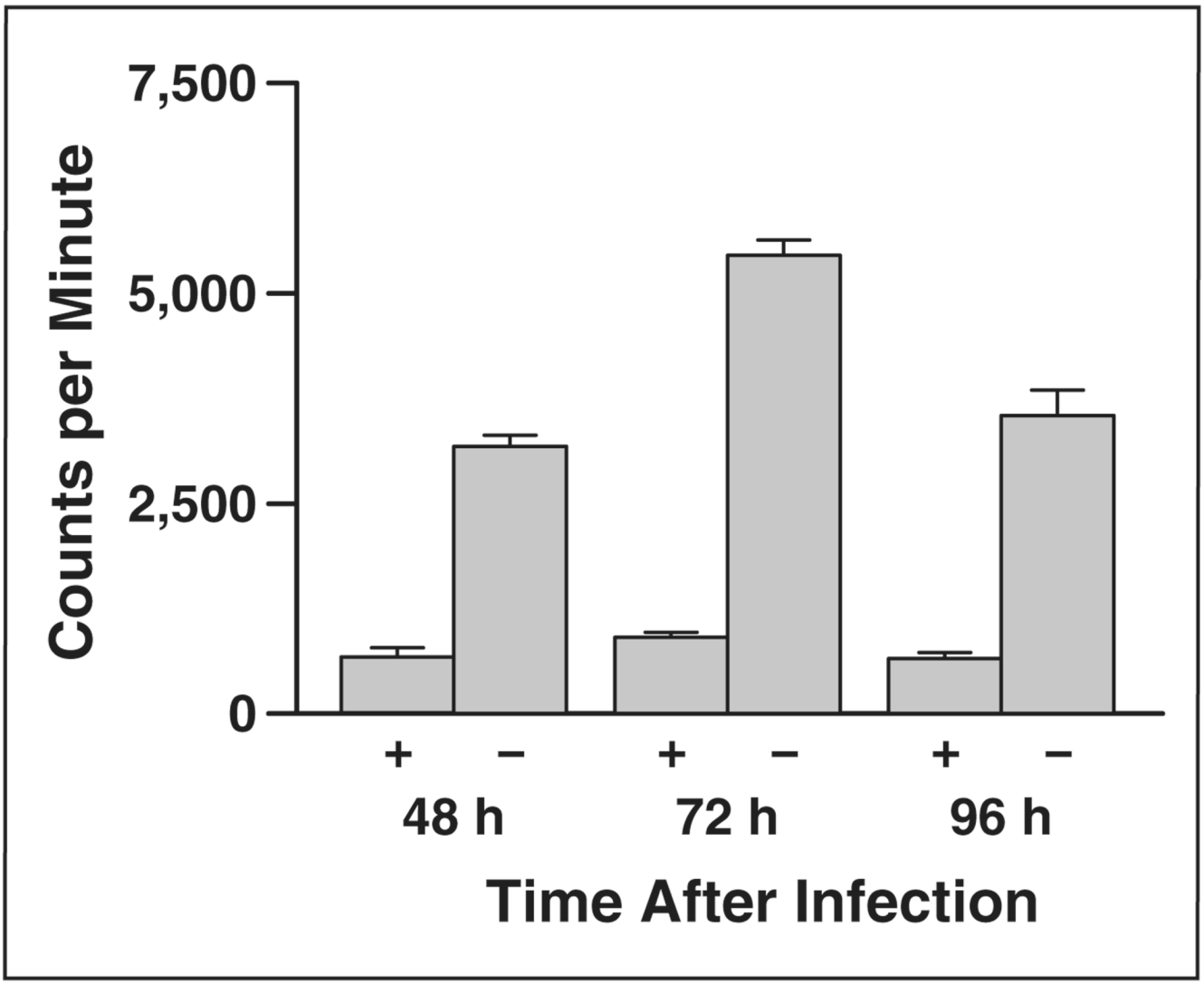

Fig. 4.

Bar graph shows radioiodine uptake by BxPC-3 pancreatic cancer cells infected with engineered measles virus expressing sodium-iodide symporter gene with (+) and without (−) 10 μmol/L of $KClO_4$, competing substrate for sodium-iodide symporter.

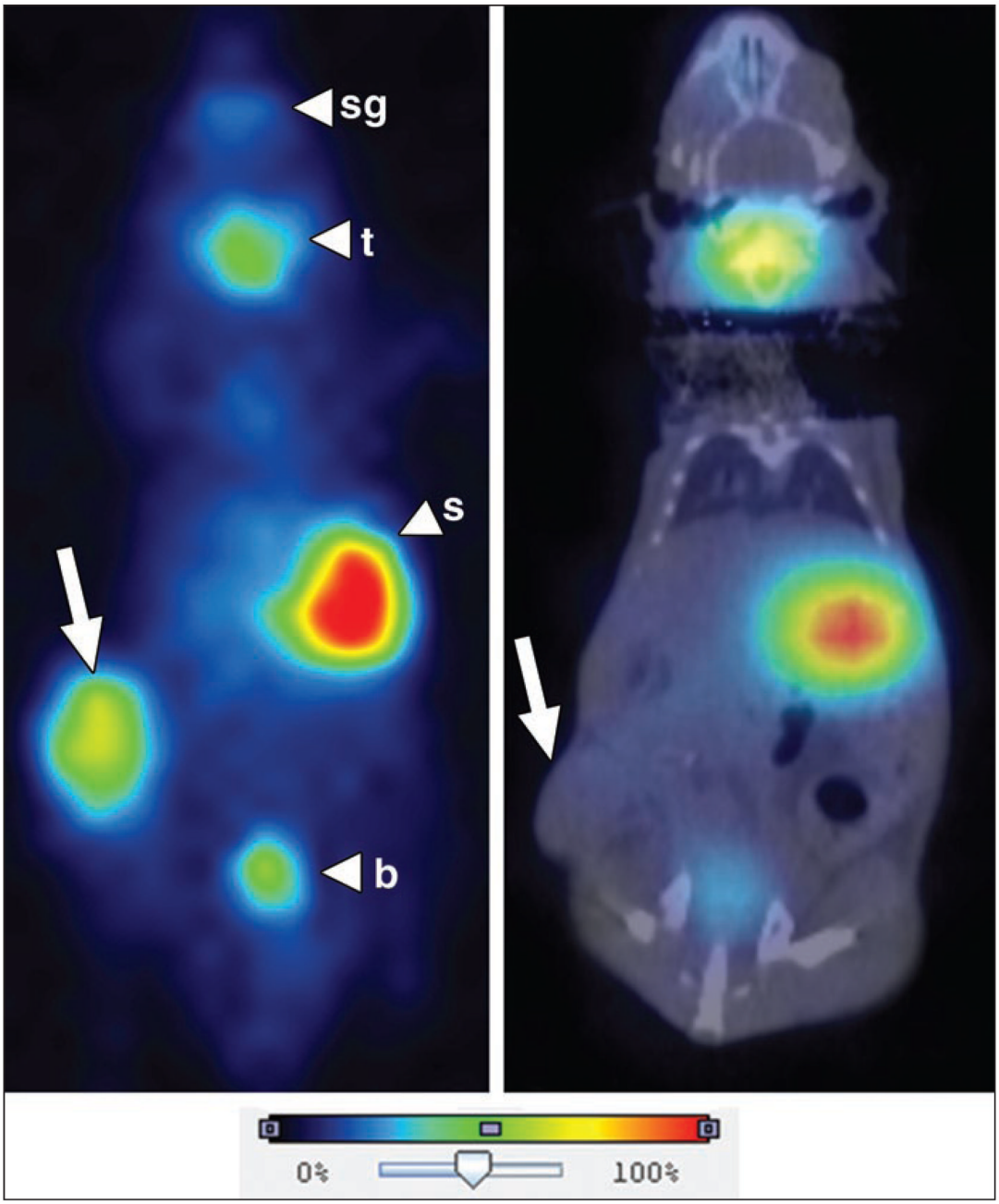

A

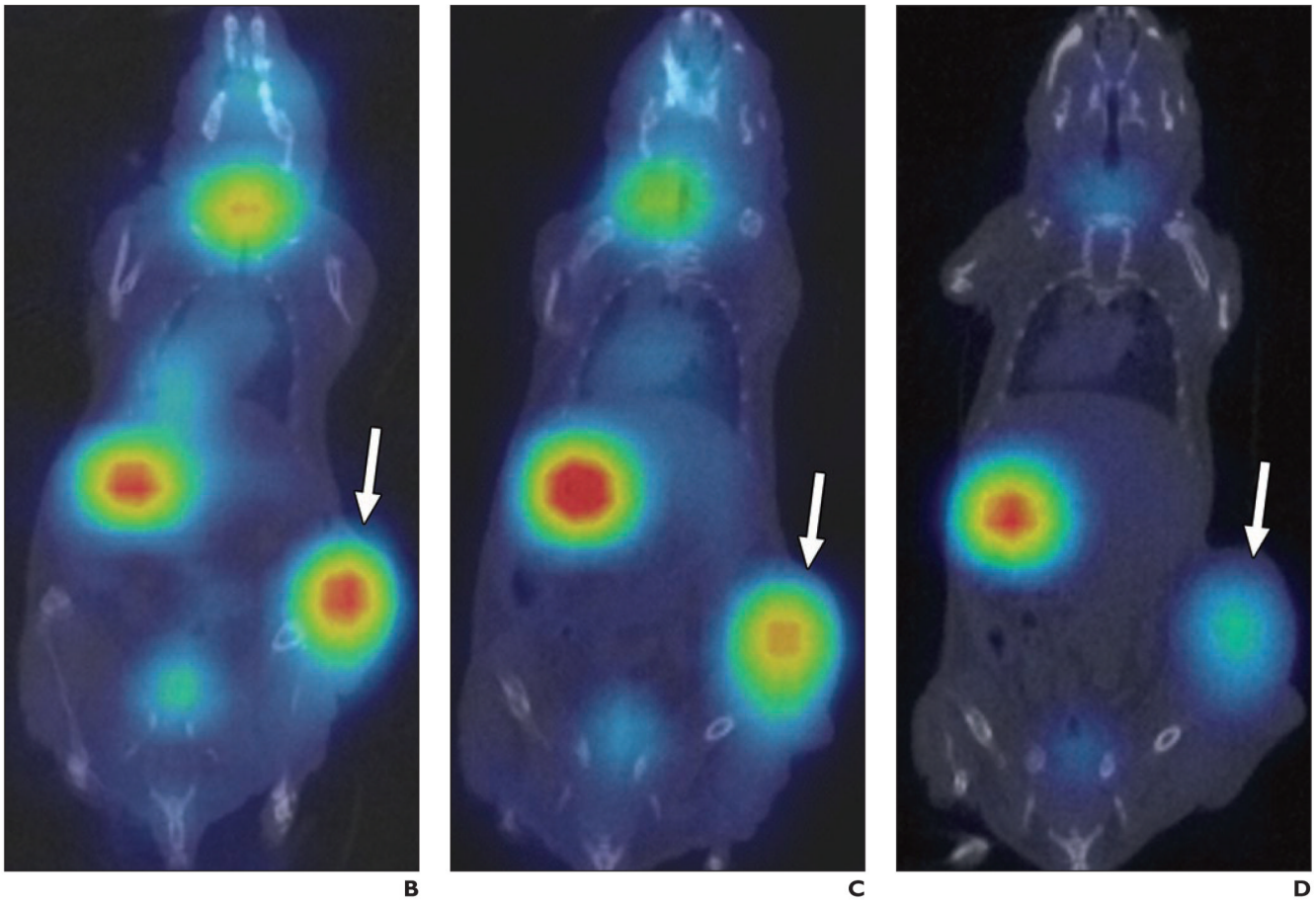

Fig. 5.

Representative ^{123}I radionuclide images of virus-treated and control tumor xenografts.

A, Planar image (*left*) shows strong intratumoral ^{123}I uptake (*arrow*) in mouse treated with engineered measles virus expressing sodium-iodide symporter gene (MV-NIS). Micro-SPECT/CT image (*right*) shows no significant intratumoral (IT) uptake in uninfected control mouse. Note other areas of physiologic uptake (*arrowheads*) in salivary glands (sg), thyroid gland (t), and stomach (s), and excretion into bladder (b).

B–D, Serial coronal fusion micro-SPECT/CT images of representative BxPC-3 tumor (*arrows*)-bearing mouse day 2 (**B**), 3 (**C**), and 5 (**D**) after IT MV-NIS injection. IT activity was maximum on day 2 (1.34 MBq; injection dose per gram of tissue [ID/g] = 11.1%) and decreased over time on day 3 (1.29 MBq; ID/g = 8.2%) and day 5 (1.05 MBq; ID/g = 7.5%). By day 8, no NIS-specific IT activity was seen (data not shown).

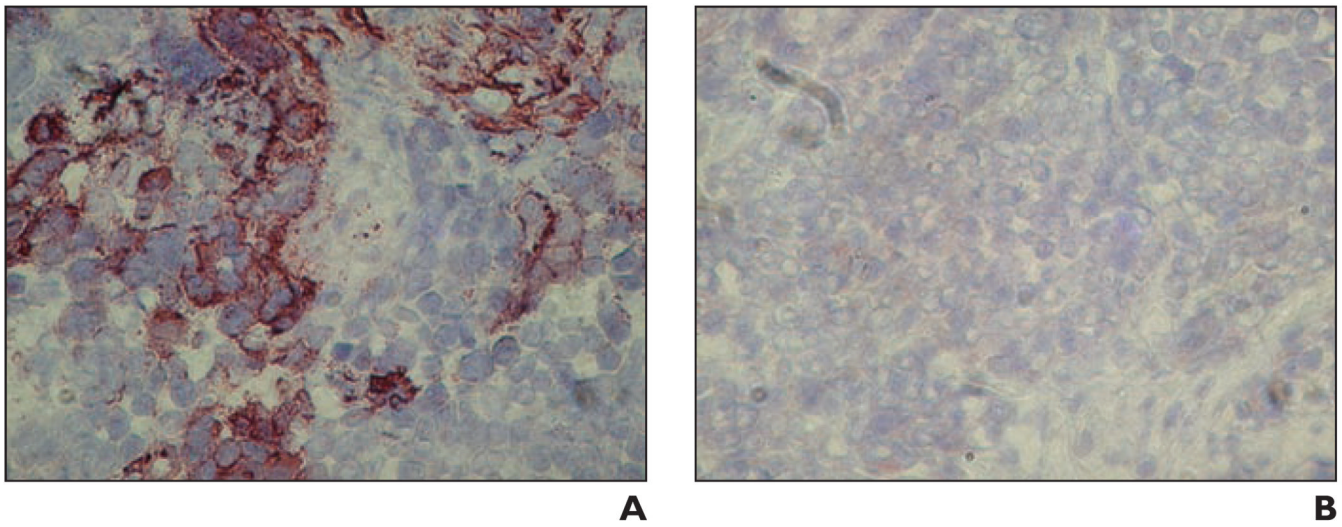

Fig. 6.

Immunohistochemical staining for measles virus nucleoprotein. Both sections were photographed at 200× magnification.

A, Section is from representative BxPC-3 tumor injected with engineered measles virus expressing sodium-iodide symporter gene (MV-NIS). Photomicrograph shows reddish-brown (Chromagen, Ferragen) punctate and heterogeneous cytoplasmic and rimlike membrane staining of tumor cells, which is consistent with measles virus infection.

B, Section is from BxPC-3 control tumor; photomicrograph shows no immunoreactivity.

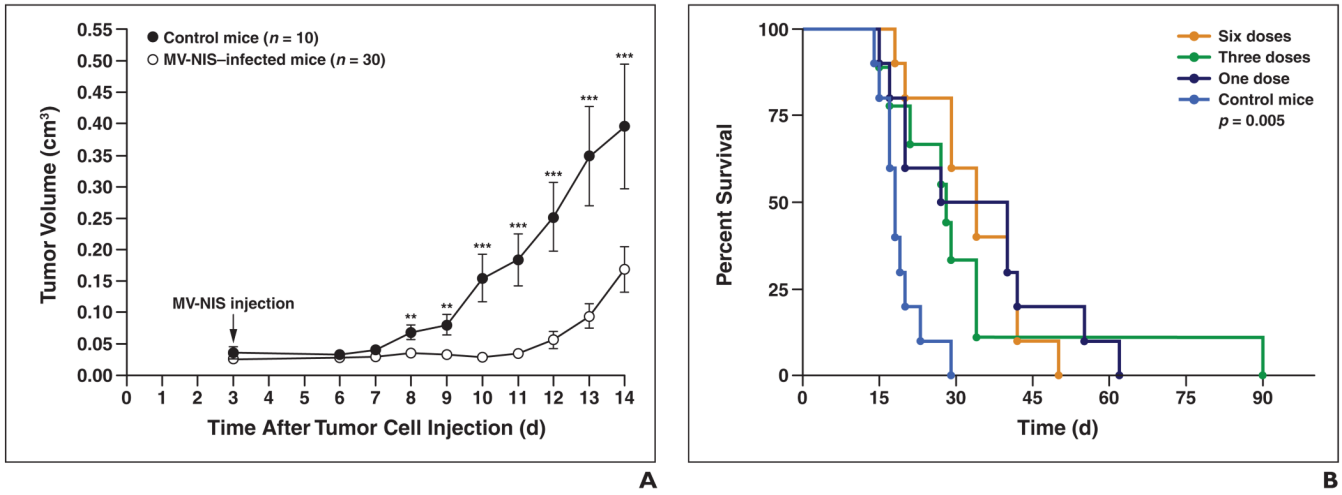

Fig. 7.

In vivo response of subcutaneous fank BxPC-3 human pancreatic cancer xenografts treated with one, three, or six doses of intratumoral (IT) engineered measles virus expressing sodium-iodide symporter gene (MV-NIS) (3.5×106 $TCID_{50}$) 2 days apart beginning day 3 after tumor cell injection. Control group mice were given three doses of IT Opti-MEM (Invitrogen). $TCID_{50}$ = tissue culture infective dose.

A, IT MV-NIS injection slows tumor growth in treated mice compared with control mice. Difference in tumor volume between control mice and treated mice (pooled data from 1, 3, and 6 MV-NIS–injected groups) is significant, observed starting on day 5 after IT MV-NIS injection. One (*), two (**), and three (***) asterisks denote *p* values < 0.05, 0.005, and 0.0005, respectively.

B, Survival curves of same mice shown in **A** reveal that IT MV-NIS therapy significantly extended survival time in treated mice versus control mice ($p = 0.005$). Number of MV-NIS injections did not affect survival.